JAIST Repository
https://dspace.jaist.ac.jp/

Title	Catalytic phosphorus and boron doping of amorphous silicon films for application to silicon heterojunction solar cells
Author(s)	Ohdaira, Keisuke; Seto, Junichi; Matsumura, Hideki
Citation	Japanese Journal of Applied Physics, 56(8S2): 08MB06-1-08MB06-5
Issue Date	2017-07-04
Type	Journal Article
Text version	author
URL	http://hdl.handle.net/10119/16138
Rights	This is the author's version of the work. It is posted here by permission of The Japan Society of Applied Physics. Copyright (C) 2017 The Japan Society of Applied Physics. Keisuke Ohdaira, Junichi Seto and Hideki Matsumura, Japanese Journal of Applied Physics, 56(8S2), 2017, 08MB06. http://dx.doi.org/10.7567/JJAP.56.08MB06
Description	

JAIST
JAPAN ADVANCED INSTITUTE OF SCIENCE AND TECHNOLOGY

Japan Advanced Institute of Science and Technology

Catalytic phosphorus and boron doping of amorphous silicon films for application to silicon heterojunction solar cells

Keisuke Ohdaira*, Junichi Seto, and Hideki Matsumura

Japan Advanced Institute of Science and Technology, Nomi, Ishikawa 923-1292, Japan

*E-mail: ohdaira@jaist.ac.jp

We investigate a novel doping method, catalytic impurity doping (Cat-doping), for application to the fabrication of silicon heterojunction (SHJ) solar cells. Thin p-type or n-type doped layers can be formed on intrinsic amorphous Si (a-Si) films by exposing P- or B-related radicals generated by the catalytic cracking of phosphine (PH_3) or diborane (B_2H_6) gas molecules. The passivation quality of underlying a-Si films can be maintained both for phosphorus (P) and boron (B) Cat-doping if we carefully choose the appropriate substrate temperature during Cat-doping. We confirm the rectifying and photovoltaic properties of an SHJ solar cell containing a B Cat-doped layer as a p-type a-Si emitter. These findings suggest the applicability of Cat-doping to SHJ solar cells.

1. Introduction

Solar power generation has recently been receiving much attention as one of the major renewable energy resources. Among many types of solar cells, wafer-based crystalline silicon (c-Si) has been utilized most widely as a photovoltaic material. Si heterojunction (SHJ) solar cells can have higher conversion efficiency than conventional homojunction c-Si solar cells, and will have more market share in the near future.[1] This is because of the higher open-circuit voltage (V_{oc}) obtained in the SHJ solar cells than in conventional c-Si solar cells, owing to good surface passivation provided by amorphous Si (a-Si) films.[2–14] A V_{oc} of as high as 750 mV has been actually realized in commercial-sized SHJ cells fabricated using a thin (<100 μm) c-Si wafer.[14]

For further improvement in the performance of SHJ solar cells, heterojunction back-contact (HBC) solar cells are extensively investigated these days.[15–17] In the HBC solar cells, all the metal electrodes and doping layers are formed on the rear surface of the cell, and thus, larger short-circuit current density (J_{sc}) can be obtained owing to the absence of shadowing loss. Masuko et al. have fabricated an HBC solar cell with an efficiency of 25.6%.[15] Moreover, an amazingly high conversion efficiency of 26.33% for a HBC solar cell has been reported very recently by Kaneka Corporation.[17] These results have clearly demonstrated the high potential of the HBC solar cell concept.

The major problem with the HBC solar cells for their industrialization is the complex fabrication process required for the formation of patterned p-type and n-type a-Si films and metal electrodes. Conventionally used photolithography is not applicable to the mass production of HBC solar cells because of high fabrication cost. A simpler fabrication process for the patterned structures must thus be developed. We have so far demonstrated that shallow boron (B)- or phosphorus (P)-doped layers can be formed by exposing c-Si surfaces to B- or P-related radicals generated by the catalytic cracking of diborane (B_2H_6) or phosphine (PH_3) gas molecules on a heated tungsten (W) catalyzing wire.[18–27] This method, catalytic impurity doping (Cat-doping), can be performed at temperatures applicable to HBC solar cells, and the doped layers formed on c-Si surfaces by Cat-doping are as shallow as <5 nm.[18] We have confirmed that Cat-doping is effective also for a-Si films; intrinsic a-Si (i-a-Si) can be converted to p-type or n-type a-Si by exposing it to B- or P-related radicals.[27] Secondary ion mass spectrometry measurements have revealed that

the B and P Cat-doped layers exist within 10–15 nm from the surfaces of a-Si films.[27] Hence, Cat-doping can significantly simplify the fabrication of HBC cells, because patterned p- and n-type a-Si layers will easily be formed by the deposition of intrinsic a-Si (i-a-Si) films and successive Cat-doping of P and B atoms onto the a-Si layer through patterned hard masks. i-a-Si will remain near the a-Si/c-Si interface if the initial i-a-Si thickness is ~20 nm, and the passivation effect may remain even after the B and P Cat-doping. We have, however, not confirmed the effect of B or P Cat-doping on the passivation ability of a-Si films. We have also not demonstrated the applicability of a Cat-doped layer to the doped layer in an actual device — an SHJ solar cell.

In this study, we investigate the effect of B and P Cat-doping of a-Si films on the passivation properties of a-Si films. We also fabricate an SHJ solar cell containing a B Cat-doped layer as an emitter layer. We have confirmed the actual operation of the SHJ solar cell showing rectifying and photovoltaic properties.

2. Experimental methods

We used 20×20 mm^2, 290-μm-thick, mirror-polished n-type c-Si(100) wafers with resistivities of 1–5 Ω·cm and a bulk minority carrier lifetime (τ_b) of >10 ms under negligible Auger recombination. The wafers were first dipped in 5% hydrofluoric acid (HF) to remove native oxide layers, and then in 4 wt% hydrogen peroxide (H_2O_2) for 30 s for the formation of ultrathin oxide layers to suppress epitaxial growth during a-Si deposition.[28,29] We then formed i-a-Si films on both sides of the c-Si wafers by catalytic chemical vapor deposition (Cat-CVD) under the conditions summarized in Table I, and annealed the samples in a Cat-CVD chamber at 350 °C for 15 min to improve the passivation quality of the a-Si films. The i-a-Si-coated c-Si wafers were dipped in 30 wt% H_2O_2 for the formation of oxide layers to prevent the etching of a-Si by atomic hydrogen during Cat-doping. This is particularly important when we perform B Cat-doping since the proper amount of H_2 should be added during Cat-doping to enhance the cracking of B_2H_6 molecules through vapor-phase reactions.[30] P and B atoms were Cat-doped on one side of a sample under the conditions summarized in Table I. A schematic of the samples is shown in Fig. 1(a). Note that we always confirmed that no film deposition occurred by radicals coming from the Cat-CVD chamber walls during Cat-doping by putting bare glass

substrates simultaneously and measuring their optical transmittance after the treatment. We also prepared the samples that were subjected to only annealing for comparison. Furthermore, the samples exposed to atomic hydrogen under the conditions shown in Table I were also formed for comparison with B Cat-doped samples. The quality of a-Si passivation films was evaluated by measuring effective minority carrier lifetime (τ_{eff}) by microwave photoconductivity decay (μ-PCD) using a pulse laser with a wavelength of 904 nm and an areal photon density of 5×10^{13} /cm^2 corresponding to an excess carrier density of ~1×10^{15} /cm^3.

We also evaluated the conductivity of a-Si films after Cat-doping. i-a-Si films with a thickness of ~20 nm deposited on Corning Eagle glass by Cat-CVD were Cat-doped with P or B after the formation of ultrathin oxide layers using H_2O_2. The conditions for a-Si deposition and P or B Cat-doping are shown in Table I. Al coplanar electrodes were then evaporated through a hard mask on the P or B Cat-doped a-Si films after removing the ultrathin oxide layers. The conductivities of the films were evaluated from their current–voltage (*I*–*V*) measurement results and by simply using an i-a-Si film thickness of 20 nm. It should be noted that the conductivities were underestimated because P and B atoms were doped nonuniformly along the depth direction and the local doping effect near the film surface must be more significant.

An SHJ solar cell with a conventional structure but containing a B Cat-doped a-Si layer was also fabricated. The structure of the SHJ cell is shown in Fig. 1(b). n/i stacked a-Si films each with a thickness of ~6 nm were deposited on the back surface of a c-Si wafer. A 20-nm-thick i-a-Si film was deposited on the front side of the c-Si, followed by B Cat-doping at a holder temperature (T_{holder}) of 350 °C. The a-Si deposition and Cat-doping conditions were summarized in Table II. We then formed indium tin oxide (ITO) films with a thickness of 80 nm by sputtering and comb-shaped silver (Ag) electrodes by screen printing and successive annealing at 200 °C on both sides of the sample. The current-density–voltage (*J*–*V*) of the SHJ cell was measured under dark and 1-sun-illuminated conditions.

3. Results and discussion

3.1 P Cat-doping

Figure 2 shows the τ_{eff} of c-Si wafers passivated with a-Si films before and after P Cat-doping at T_{holder} values of 100–350 °C, as well as the τ_{eff} of the samples subjected to only post-deposition annealing at the same temperature and duration as those in P Cat-doping. τ_{eff} values of 3–4 ms are confirmed before P Cat-doping, indicating the excellent passivation quality of Cat-CVD a-Si films. τ_{eff} decreases to ~1 ms after P Cat-doping at a T_{holder} of 100 °C. A decrease in τ_{eff} is also observed when the sample is simply annealed at 100 °C, but more significant reduction in τ_{eff} is confirmed in the case of P Cat-doping. This indicates that P Cat-doping at a T_{holder} of 100 °C deteriorates the passivation quality of the a-Si film. One possible reason for the degradation of passivation quality is the etching of a-Si films by atomic hydrogen. Atomic hydrogen is generated through the catalytic decomposition of PH_3 molecules—$PH_3 \rightarrow P + 3H$,[31–33] which may etch the a-Si film and reduce its thickness. We have actually confirmed a reduction in the thickness of a-Si after P Cat-doping from ~20 nm to ~12 nm. Such a reduction in the thickness of the a-Si film may lead to the deterioration of its doping effect and passivation quality. Moreover, the conductivity of a-Si after P Cat-doping at a T_{holder} of 100 °C was 1.5×10^{-9} S/cm, which is insufficient for device application. The reason for the decrease in τ_{eff} after simple annealing at 100 °C is unclear at present. A similar reduction in τ_{eff} is seen in the case of P Cat-doping at a T_{holder} of 200 °C. The degree of reduction in τ_{eff} is, however, highly suppressed, and τ_{eff} remains >3 ms even after P Cat-doping. We have also confirmed a reduction in the thickness of a-Si by Cat-doping at a T_{holder} of 200 °C similarly to the case for P Cat-doping at a T_{holder} of 100 °C. The smaller reduction in τ_{eff} might be explained by the more effective termination of defects on the a-Si/c-Si interface by hydrogen atoms. The conductivity of a-Si after P Cat-doping (5.9×10^{-10} S/cm) is still quite low, and better P Cat-doping conditions should be determined.

Figure 2(c) shows the τ_{eff} of c-Si wafers passivated with a-Si films before and after P Cat-doping at a T_{holder} of 350 °C. Unlike in the case of P Cat-doping at a lower T_{holder}, τ_{eff} is rather increased by P Cat-doping at a T_{holder} of 350 °C, and a markedly high τ_{eff} of more than 5 ms is obtained. This improvement in τ_{eff} cannot be explained by the annealing effect during P Cat-doping, since the sample subjected to only annealing at 350 °C does not show any τ_{eff} improvement. One possible reason for the τ_{eff} increase is the termination of defects on the a-Si/c-Si interface by hydrogen atoms, as mentioned above. Another possible

explanation is the downward band bending caused by the formation of n-type a-Si through P Cat-doping. Such a modification of band alignment can decrease the density of minority carriers — holes — near the a-Si/c-Si interface and recombination rate. The important finding here is that there exists a condition for P Cat-doping under which the passivation quality of an underlying a-Si film does not deteriorate and is rather improved. The conductivity of a-Si after P Cat-doping at a T_{holder} of 350 °C was 5.9×10^{-8} S/cm. This value is much higher than those of a-Si films after P Cat-doping at a lower T_{holder}; however, it is still insufficient for the application of P Cat-doping to actual SHJ solar cells. Further optimization of the conditions for P Cat-doping is necessary.

3.2 B Cat-doping

Figure 3 shows the τ_{eff} of c-Si wafers passivated with a-Si films before and after B Cat-doping at T_{holder} values of 100–350 °C. We here also show the τ_{eff} values of the samples only after annealing at the same temperatures as those for Cat-doping and after hydrogen treatment for comparison. A marked reduction in τ_{eff} to much less than 1 ms is seen in the case of B Cat-doping and H treatment at a T_{holder} of 100 °C. τ_{eff} is also decreased by B Cat-doping or H treatment at a T_{holder} of 200 °C, but the degree of reduction in τ_{eff} is less significant than that in the case of treatment at a T_{holder} of 100 °C. Such drastic reductions in τ_{eff} may be due to the etching of a-Si films by atomic hydrogen, in spite of surface protection by the thin oxide layers formed during H_2O_2 dipping prior to B Cat-doping or H treatment. The etching of Si by atomic hydrogen occurs more significantly at a lower T_{holder},[34] and the greater reduction in τ_{eff} at a lower T_{holder} shown in this study is qualitatively reasonable. The conductivities of a-Si after B Cat-doping were measured to be 3.5×10^{-10} S/cm at a T_{holder} of 100 °C and 3.5×10^{-9} S/cm at a T_{holder} of 200 °C. Such low conductivities may also be related to the serious etching of a-Si by hydrogen atoms, since Cat-doped B atoms tend to be localized near the surface and the removal of the highly doped region will drastically reduce the conductivity of a-Si.

Figure 3(c) shows the τ_{eff} of c-Si wafers passivated with a-Si films before and after B Cat-doping at T_{holder} of 350 °C. The τ_{eff} values remain sufficiently high (~3 ms), unlike in the case of B Cat-doping at a lower T_{holder}. This may be due to the suppression of Si etching at a higher process temperature.[34] Note that τ_{eff} improves in the case of P Cat-doping at a

T_{holder} of 350 °C, as mentioned above. One possible reason for the unchanged τ_{eff} after B Cat-doping is the absence of the beneficial field effect. The formation of the B Cat-doped layer in a-Si leads to upward band bending, which results in the accumulation of minority carriers, i.e., holes, near the a-Si/c-Si interface. It should be emphasized that p-a-Si in particular has poorer thermal tolerance than n- and i-a-Si, and the annealing of a p-a-Si/i-a-Si stack at 350 °C generally results in the serious deterioration of the passivation quality of this stack owing to a marked hydrogen release.[35] The rather better passivation quality at a higher T_{holder} after B Cat-doping might be due to the introduction of hydrogen during B Cat-doping. B Cat-doping at such a high T_{holder} also contributes to the increase in the conductivity of a-Si films. The a-Si film after B Cat-doping shows a conductivity of 1×10^{-6} S/cm. One reason for the higher conductivity is the more efficient doping and activation of B atoms. It should be mentioned that B_2H_6 can also be thermally decomposed at a temperature of >300 °C,[36, 37] and B doping can take place also through the thermal decomposition on the a-Si surface.[27] This thermal decomposition process also increase the conductivity of the a-Si film. This markedly high conductivity may be applicable to the emitter of an SHJ solar cell, and we attempted to fabricate an actual device.

3.3 Application of B Cat-doped layer to an SHJ solar cell

Figure 4 shows the *J*–*V* characteristics of the SHJ solar cell containing a p-type a-Si emitter layer formed through B Cat-doping, whose structure is schematically shown in Fig. 1(b). The fabricated device shows clear rectifying and photovoltaic properties, and the p-type a-Si layer formed by B Cat-doping successfully acts as an emitter layer. The low J_{sc} is due to an untextured c-Si surface and the resulting large optical reflection loss as well as a serious parasitic absorption in a-Si located on the illuminated side. The low V_{oc} observed in the SHJ cell (~0.4 V) is probably not due to the deterioration of interface quality by B Cat-doping, since a markedly high τ_{eff} of >3 ms is observed in the sample after the doping process. Note that we have obtained a V_{oc} of >0.68 V in a reference cell, in which a p-type a-Si film deposited by Cat-CVD with a conductivity of 5×10^{-4} S/cm was used.[28] Insufficient B doping concentration and/or depth may be the reason for the low V_{oc} and an increase in V_{oc} will be realized by further optimization of B Cat-doping.

Cat-CVD can be used to form Si nitride (SiN_x) films with excellent passivation

quality,[24, 38, 39] which will be utilized in the front-side passivation films of HBC solar cells. The sufficient passivation of rear-side c-Si surface in HBC cells can be achieved by using Cat-CVD i-a-Si films, as demonstrated in previous work[28, 29] as well as in this paper. If Cat-doping realizes the formation of patterned n-type and p-type a-Si regions, the simple fabrication of HBC solar cells with high performance will be established.

4. Conclusions

We have investigated the effect of P and B Cat-doping on the passivation quality of a-Si films. Cat-doping at higher T_{holder} values leads to better τ_{eff} both for P and B Cat-doping. τ_{eff} is rather improved by P Cat-doping and is maintained after B Cat-doping at a T_{holder} of 350 °C. A sufficiently high substrate temperature during Cat-doping is thus important to keep the initial passivation quality of a-Si films after Cat-doping. We have also fabricated an SHJ solar cell with a p-type a-Si emitter formed by B Cat-doping and confirmed its rectifying and photovoltaic properties. These results demonstrate the feasibility of fabricating SHJ and HBC solar cells with doped a-Si regions formed through Cat-doping.

Acknowledgment

This work was supported by the Core Research for Evolutional Science and Technology (CREST), Japan Science and Technology Agency (JST) program and JSPS KAKENHI Grant Number 16K14400.

References

1) International Technology Roadmap for Photovoltaic (ITRPV) 2015 Results including Maturity Reports [http://www.itrpv.net/Reports/Downloads/2016/].
2) S. De Wolf, A. Descoeudres, Z. C. Holman, and C. Ballif, Green **2**, 7 (2012).
3) J. L. Hernandez, D. Adachi, D. Schroos, N. Valckx, N. Menou, T. Uto, M. Hino, M. Kanematsu, H. Kawasaki, R. Mishima, K. Nakano, H. Uzu, T. Terashita, K. Yoshikawa, T. Kuchiyama, M. Hiraishi, N. Nakanishi, M. Yoshimi, and K. Yamamoto, Proc. 28th European Photovoltaic Solar Energy Conf., 2013, p. 741.
4) A. Descoeudres, Z. C. Holman, L. Barraud, S. Morel, S. De Wolf, and C. Ballif, IEEE J. Photovoltaics **3**, 83 (2013).
5) F. Jay, D. Muñoz, T. Desrues, E. Pihan, V. A. de Oliveira, and N. Enjalbert, Sol. Energy Mater. Sol. Cells **130**, 690 (2014).
6) K. Nakada, J. Irikawa, S. Miyajima, and M. Konagai, Jpn. J. Appl. Phys. **54**, 052303 (2015).
7) H. Fujiwara, H. Sai, and M. Kondo, Jpn. J. Appl. Phys. **48**, 064506 (2009).
8) M. Taguchi, E. Maruyama, and M. Tanaka, Jpn. J. Appl. Phys. **47**, 814 (2008).
9) J. Ziegler, A. Montesdeoca-Santana, D. Platt, S. Hohage, R. GuerreroLemus, and D. Borchert, Jpn. J. Appl. Phys. **51**, 10NA03 (2012).
10) D. Thibaut, De V. Sylvain, S. Florent, D. Djicknoum, M. Delfina, G.-F. Marie, K. Jean-Paul, and R. Pierre-Jean, Energy Procedia **8**, 294 (2011).
11) A. Tomasi, B. Paviet-Salomon, D. Lachenal, S. M. de Nicolas, A. Descoeudres, J. Geissbuhler, S. De Wolf, and C. Ballif, IEEE J. Photovoltaics **4**, 1046 (2014).
12) Z. Shu, U. Das, J. Allen, R. Birkmire, and S. Hegedus, Prog. Photovoltaics **23**, 78 (2015).
13) N. Mingirulli, J. Haschke, R. Gogolin, R. Ferré, T. F. Schulze, J. Düsterhöft, N.-P. Harder, L. Korte, R. Brendel, and B. Rech, Phys. Status Solidi: Rapid Res. Lett. **5**, 159 (2011).
14) M. Taguchi, A. Yano, S. Tohoda, K. Matsuyama, Y. Nakamura, T. Nishiwaki, K. Fujita, and E. Maruyama, IEEE J. Photovoltaics **4**, 96 (2014).
15) K. Masuko, M. Shigematsu, T. Hashiguchi, D. Fujishima, M. Kai, N. Yoshimura, T. Yamaguchi, Y. Ichihashi, T. Mishima, N. Matsubara, T. Yamanishi, T. Takahama, M. Taguchi, E. Maruyama, and S. Okamoto, IEEE J. Photovoltaics **4**, 1433 (2014).
16) J. Nakamura, N. Asano, T. Hieda, C. Okamoto, H. Katayama, and K. Nakamura, IEEE J.

Photovoltaics **4** 1491 (2014).
17) http://www.nedo.go.jp/english/news/AA5en_100109.html
18) H. Matsumura, T. Hayakawa, T. Ohta, Y. Nakashima, M. Miyamoto, Trinh Cham Thi, K. Koyama, and K. Ohdaira, J. Appl. Phys. **116**, 114502 (2014).
19) H. Matsumura, M. Miyamoto, K. Koyama, and K. Ohdaira, Sol. Energy Mater. Sol. Cells **95**, 797 (2011).
20) T. Hayakawa, Y. Nakashima, M. Miyamoto, K. Koyama, K. Ohdaira, and H. Matsumura, Jpn. J. Appl. Phys. **50**, 121301 (2011).
21) T. Hayakawa, Y. Nakashima, K. Koyama, K. Ohdaira, and H. Matsumura, Jpn. J. Appl. Phys. **51**, 061301 (2012).
22) T. Hayakawa, M. Miyamoto, K. Koyama, K. Ohdaira, and H. Matsumura, Thin Solid Films **519**, 4466 (2011).
23) T. Hayakawa, T. Ohta, Y. Nakashima, K. Koyama, K. Ohdaira, and H. Matsumura, Jpn. J. Appl. Phys **51**, 101301 (2012).
24) Trinh Cham Thi, K. Koyama, K. Ohdaira, and H. Matsumura, J. Appl. Phys. **116**, 044510 (2014).
25) T. Ohta, K. Koyama, K. Ohdaira, and H. Matsumura, Thin Solid Films **575**, 92 (2015)
26) S. Tsuzaki, K. Ohdaira, T. Oikawa, K. Koyama, and H. Matsumura, Jpn. J. Appl. Phys. **54**, 072301 (2015).
27) J. Seto, K. Ohdaira, and H. Matsumura, Jpn. J. Appl. Phys **55**, 04ES05 (2016).
28) T. Oikawa, K. Ohdaira, K. Higashimine, and H. Matsumura, Curr. Appl. Phys. **15**, 1168 (2015).
29) K. Ohdaira, T. Oikawa, K. Higashimine, and H. Matsumura, Curr. Appl. Phys. **16**, 1026 (2016).
30) H. Umemoto, T. Kanemitsu, and A. Tanaka, J. Phys. Chem. A **118**, 5156 (2014).
31) H. Umemoto, Y. Nishihara, T. Ishikawa, and S. Yamamoto, Jpn. J. Appl. Phys. **51**, 086501 (2012).
32) H. Umemoto, T. Kanemitsu, and Y. Kuroda, Jpn. J. Appl. Phys. **53**, 05FM02 (2014).
33) H. Umemoto, Thin Solid Films **575**, 9 (2015).
34) K. Kamesaki, A. Masuda, A. Izumi, and H. Matsumura, Thin Solid Films **395**, 169 (2001)
35) S. De Wolf and M. Kondo, J. Appl. Phys. **105**, 103707 (2009).

36) P. Roca i Cabarrocas, S. Kumar, and B. Drevillon, J. Appl. Phys. **66**, 3286 (1989).
37) H. Habuka, S. Akiyama, T. Otsuka, and W. F. Qu, J. Cryst. Growth **209**, 807 (2000).
38) Trinh Cham Thi, K. Koyama, K. Ohdaira, and H. Matsumura, Jpn. J. Appl. Phys. **53**, 022301 (2014).
39) Trinh Cham Thi, K. Koyama, K. Ohdaira, and H. Matsumura, Jpn. J. Appl. Phys. **55**, 02BF09 (2016).

Figure Captions

Fig. 1. (Color online) Schematic sample structures for (a) τ_{eff} measurement and (b) an SHJ solar cell.

Fig. 2. (Color online) τ_{eff} of c-Si wafers passivated with a-Si films before and after P Cat-doping at T_{holder} values of (a) 100, (b) 200, and (c) 350 °C. τ_{eff} of the sample with only post-deposition annealing at the same temperature and duration as the P Cat-doping is also shown for comparison.

Fig. 3. (Color online) τ_{eff} of c-Si wafers passivated with a-Si films before and after B Cat-doping at T_{holder} values of (a) 100, (b) 200, and (c) 350 °C. τ_{eff} values of the sample with only post-deposition annealing and only H_2 treatment at the same temperature and duration as those for B Cat-doping are also shown for comparison.

Fig. 4. *J-V* characteristics of an SHJ solar cell with a B Cat-doped p-type layer under dark and 1-sun-illuminated conditions.

Table I Conditions of intrinsic a-Si deposition, H treatment, and Cat-doping for the preparation of the samples for τ_{eff} measurement.

	T_{holder} (°C)	T_{cat} (°C)	Duration (s)	Pressure (Pa)	Gas	Flow rate (sccm)
i-a-Si deposition	125	1800	90	1	SiH_4	10
H treatment	100–350	1800	600	1	H_2	20
B doping	100–350	1800	600	3.9	2.25% B_2H_6	20
					H_2	40
P doping	100–350	1500	1800	2	2.25% PH_3	20

Table II Conditions of a-Si deposition and B Cat-doping for the fabrication of an SHJ solar cell.

	T_{holder} (°C)	T_{cat} (°C)	Pressure (Pa)	Gas	Flow rate (sccm)
i-a-Si deposition	125	1800	1	SiH_4	10
n-a-Si deposition	250	1800	2	SiH_4 2.25% PH_3	10 4.4
B doping	350	1800	3.9	2.25% B_2H_6 H_2	20 40

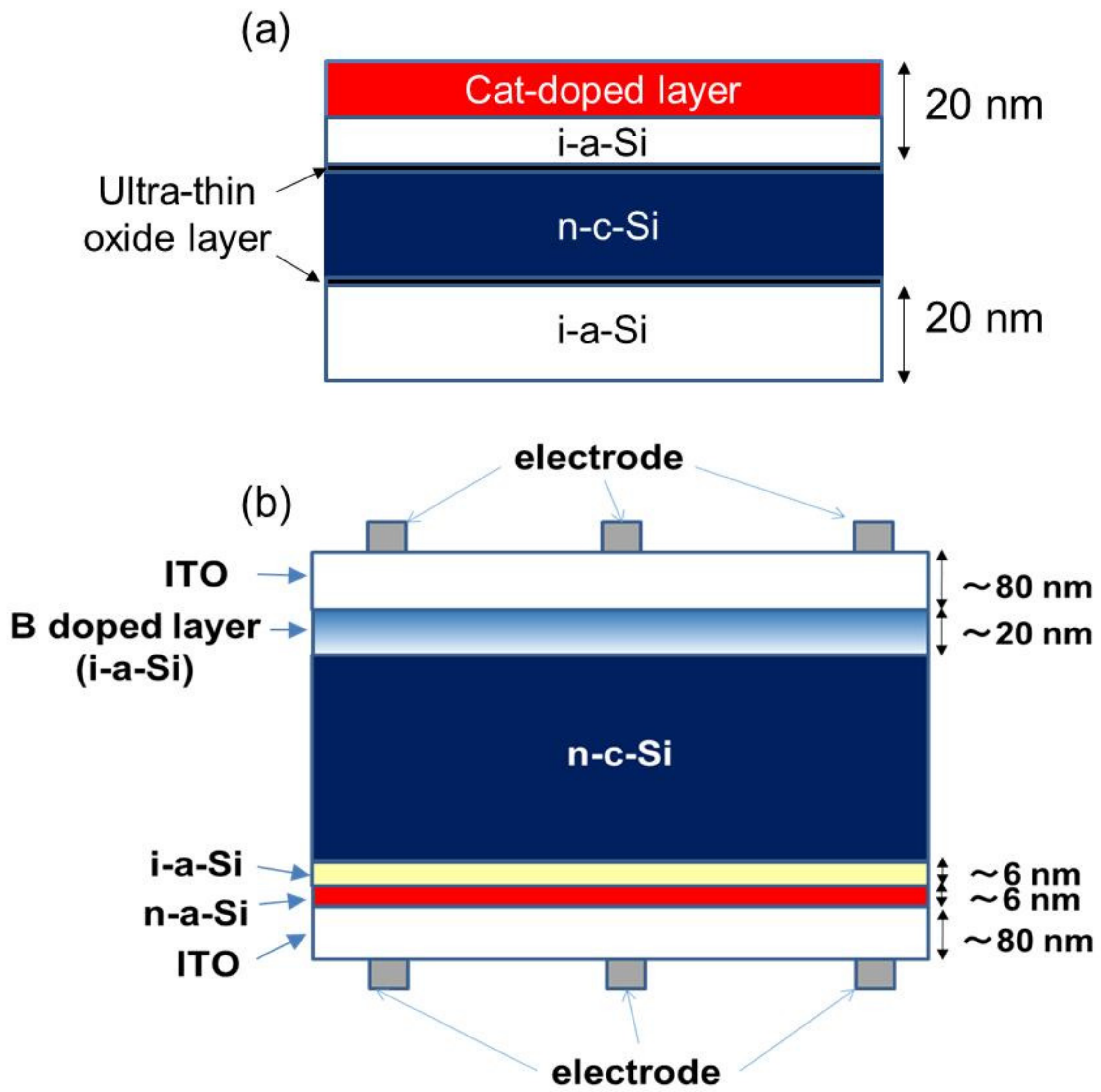

Fig. 1. (Color online)

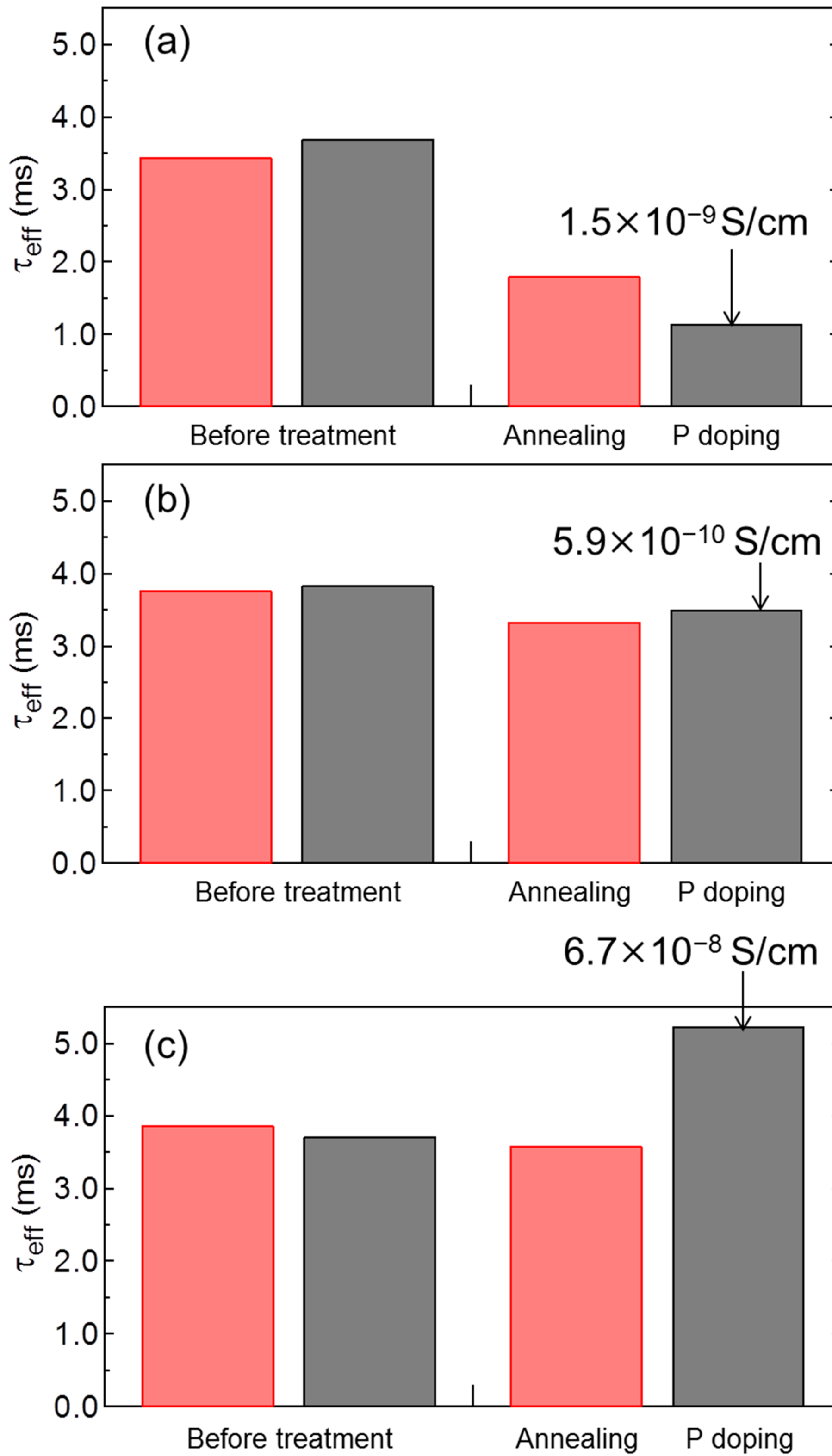

Fig. 2. (Color online)

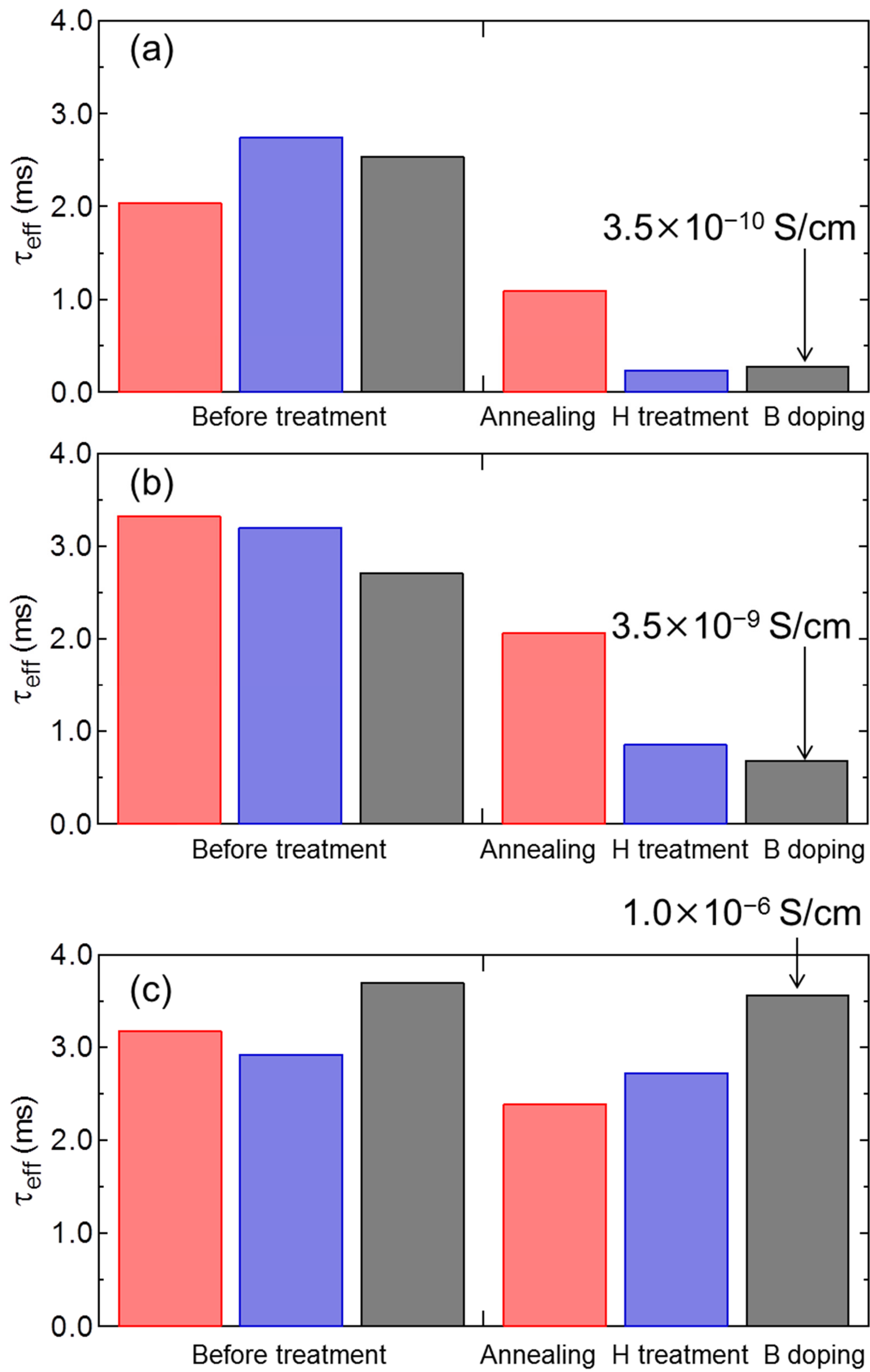

Fig. 3. (Color online)

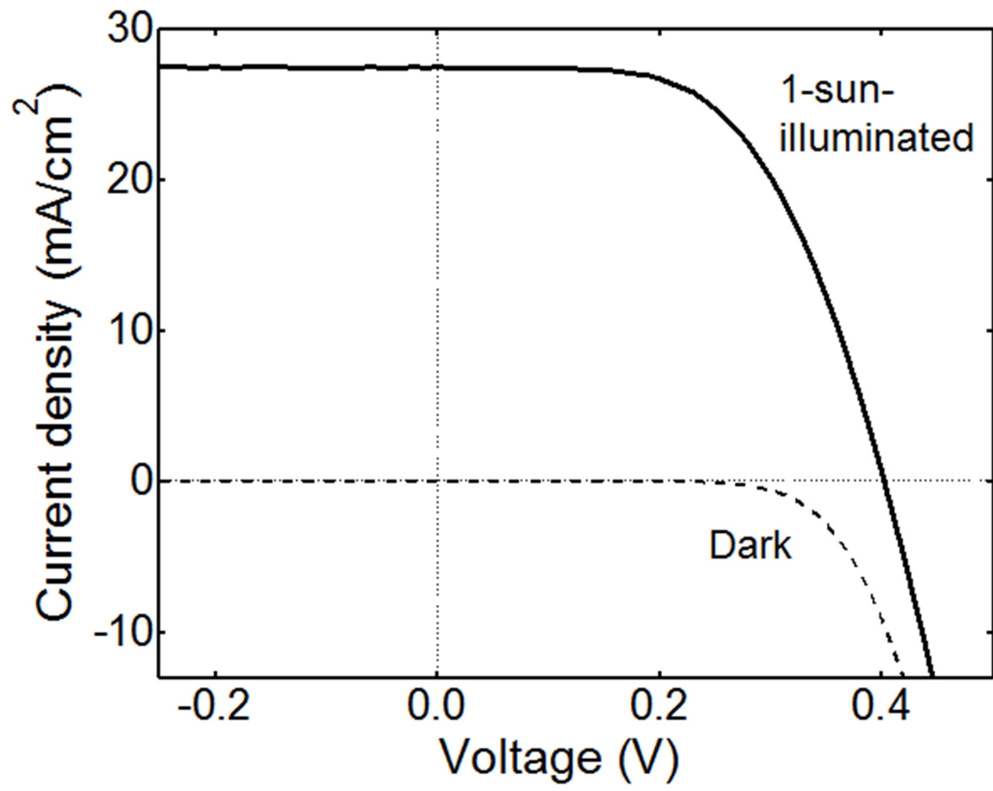

Fig. 4.